[1]Kalyan Singh

[2]Sumit Saroha

[3]Avnesh Verma

Performance Comparison of PID & FOPID for Solar PV & Wind Power Grid Integration

Abstract: - his paper presents performance analysis of grid connected solar photovoltaic (PV) and wind power plants with an aim to analyze the stability of system. The work evaluates the performance of Proportional-Integral-Derivative (PID) and Fractional Order PID (FOPID) controllers by utilizing three different algorithms like: Firefly (FF), Whale Optimization Algorithm (WOA), and Path Finder (PF). These techniques are used for optimal tuning of controller parameters such as: *Kp, Ki, Kd,* λ and μ. The performance of each technique is tested under three different cases depending on solar irradiance and wind speed. In Case I, Solar Irradiance is 850 W/m^2 & Wind Speed is 15 ms, in Case II, Solar Irradiance is 900 W/m^2 & Wind Speed is 10 ms and in Case III, output is analyzed at Solar Irradiance of 1000 W/m^2 and Wind Speed is 15 ms. There is performance comparison on DC link voltage and output voltage of proposed system on their responses to critically assess the efficacy in optimizing power generation with stable grid operation. The results proved the superiority of FOPID controllers as compared to PID controllers in terms of stability and settling time. Further, WOA-FOPID offers a shortest settling time of 0.28 seconds amongst all FOPID controllers for the case

Keywords: Controller, FOPID, Grid Integration, Tuning Algorithm

I.   INTRODUCTION

The integration of renewable energy sources such as: solar photovoltaic (PV) and wind power, into existing electrical grids is pertinent in maintaining transition towards achieving sustainable eco-systems at a faster pace [1]. The variable and intermittent nature of these renewable sources poses significant challenges for an engineer to maintain the grid stability and reliability. Therefore, the effective control strategies are very crucial for addressing these challenges for ensuring the seamless integration of renewable energy into the grid [2]-[3]. There are two promising approach involved in it for maintaining the same so first one is Proportional-Integral-Derivative (PID) [4] and second one is Fractional-Order Proportional-Integral-Derivative (FOPID) controller [5]. These controllers are quite essential for maintaining the dynamic behavior of power systems by improving the performance of power electronic converters to ensure the stability of renewable energy integrated grid [6].

The solar PV and wind hybrid system of 1 KW is integrated with single phase grid using PI controller to reduce the Total Harmonic Distortion (THD). The Kp and Ki has been computed through heuristic tuning method and achieves THD value of 2.54% at a settling time of 0.5 seconds [7]. The performance DSP-based current controller with LCL filter is investigated for grid-connected PV inverters to minimize the distortion. It calculates the duty cycle to generate Pulse Width Modulation (PWM) pulses for triggering the H-bridge converters and it achieves the sine wave at a Settling time of 2 cycles under average steady-state error of 0.45A [8]. For handling the power quality issues under maximum power point tracking algorithm (MPPT), a novel Fuzzy and neural network based Luo converter has been implemented on single phase solar PV & wind integrated system. The value of THD under various testing conditions is 3.18% using PI controller [9]. In ref. [10], modified P&O based MPPT controller has been proposed for a single-phase grid-integrated photovoltaic (PV) system which is not only adaptive for isolated but also for grid-connected modes. In former, PV inverter maintains the voltage amplitude and frequency at the load end and operates under voltage control mode. Conversely, in later mode, inverter maintains amplitude and frequency of its output voltage and operates under current control mode. It maintains the grid synchronization using a PLL, with a synchronization settling time of 20 ms.

Ant Colony Optimization (ACO) is used for parameters optimization of adaptive neuro-fuzzy inference system (ANFIS) based FOPID which is implemented on DC motor driven Electric vehicles (EVs) speed tracking.

[1,2]Department of Electrical and Electronics Engineering, Guru Jambheshwar University of Science & Technology, Hisar, India

[3]Department of Instrumentation, Kurukshetra University, Kurukshetra

Corresponding author: Sumit Saroha

Email: saroha_sumit0178@yahoo.com

The accuracy in terms of mean absolute error is 0.004 [11]. Gradient-Based Optimization (GBO) algorithm is adopted for FOPID tuning & used as a controller for Automatic Voltage Regulator (AVR) designing. The value of settling time is 0.738 second [12]. Ant Lion Optimization (ALO) used for optimal tuning of FOPID based controller [13]. The cascaded structure of PID parameters has been tuned via Local Unimodal Sampling (LUS) and the Spotted Hyena Optimizer (SHO). The Settling time is taken to be 0.1 s by the controller to control the speed of switched reluctance motor [14]. For the control performance improvement of micro gas turbine, hybrid algorithm based on improved Particle Swarm Optimization (PSO) algorithm and cuckoo search algorithm has been proposed for tuning the parameters of fuzzy based PID controller. The settling time taken under 5% load distribution is 1.4 seconds [15]. Therefore, there is need to explore implementation procedure of PID and FOPID controllers for grid integration of solar PV and wind power system. These are the following major contribution of this work:

> Compare the performance of PID and FOPID controllers in managing the output voltage at the bus and the inverter end connected to grid.
> Proposes three different algorithms called FF, WOA & PF for optimal tuning of parameters for both PID and FOPID in order to resolve the issues related to optimization.
> The performance of every approach is tested under three different cases of Solar Irradiance & Wind Speed so that its efficacy can be tested under dynamic response to obtain considerable stability.

The presentation of paper is explained as: Section 2 gives the detailed description of PID and FOPID controllers. Section 3 has details about the theory of tuning algorithm used, Section 4 gives the detailed results and discussion about present work and Section 5 concludes the present work.

II. STRUCTURE OF CONTROLLERS USED

In this section, the basic structures used (PID and FOPID) for presented work is discussed. The details of the discussion are as follows as:

A. PID Controller

In this section, the basic structures used (PID and FOPID) for presented work is discussed. The details of the discussion are as follows as: The most common structures for designing a PID controller are parallel and series connections types. In the former all Proportional (P), Integral (I), and Derivative (D) are connected in such a way that they will make a parallel connections and they are operated separately through the equations [16]. These individual actions performed by all are combined at a summation point for producing the overall controlled output response. The parameters for each component are independent therefore, they require separate tuning for getting the better output response [17]. The overall control action can be mathematically represented by the equations given below:

$$u(t) = K_p e(t) + K_i \int e(t)dt + K_d \frac{de(t)}{dt} \tag{1}$$

In above (1), Kp, Ki & Kd are the representation for proportional, integral, and derivative gains, respectively, and $e(t)$ represents the produced error signal. In the series type PID controller, the equations are originating from pneumatic control and circuit characteristics are analog one. Unlike the parallel type, changes in the proportional gain of each controller affect all above three actions of PID [18]. Additionally, the gain of proportional is influenced by the gains of integral and derivative.

$$e_1(t) = e(t) + T_d \frac{de(t)}{dt}$$

$$u(t) = K_c \left(e(t) + \frac{1}{T_i} \int e(t)dt \right) \tag{2}$$

In the above series type PID controller, the gain Kc, have influenced all three PID components. The integral parameter Ti, along with derivative tuning parameter Td affects the proportional term. By adjusting Td, there is impact on derivative and proportional actions, while by modifying Ti, there is influence on integral and proportional actions. Hence, in the interconnected system of PID variation in one parameter can significantly affect the overall control dynamics. The figure 1 shows the architecture representation of conventional PID Controller [19].

B.   FOPID Controller

In the proposed system, there is hybridization of Solar PV and Wind power with grid (single phase). The hybridization imposes the extra burden on power and control engineers as it may leads to problem of synchronization. However, the hybridization can reduce the overall cost of standalone power system by providing alternate energy option to electricity supply system and as a result of this efficiency of system is enhanced. The output power of solar PV is DC which feeds to the DC-DC converter and on the other hand, the output of wind turbine is AC which is fed to a rectifier unit integrated with single phase grid. Therefore, to regulate the DC bus output voltage connected to the grid, it is essential to propose a finely tuned and robust FOPID controller which is extended version of classical PID by incorporating integrators and differentiators of non-integer orders [20]. This design allows optimal tuning with less sensitivity to parameter changes in the integrated system. The emergence of fractional calculus has enabled the transition to fractional-order dynamic models and controllers, in return enhancing system robustness. Figure 2 shows the architecture of FOPID Controller for Proposed System [21] [22]. The transfer function of the FOPID controller is defined as follows:

$$G_c(s) = \frac{U(s)}{E(s)} = K_P + K_I s^{-\lambda} + K_D s^{\mu} \tag{3}$$

In above (3), λ and μ are fractional orders of integrator and differentiator. Primary goal of a FOPID controller is to improve time and frequency response of the control system with the help of appropriately setting of the FOPID parameters such as: *Kp*, *Ki*, *Kd*, λ and μ [23].
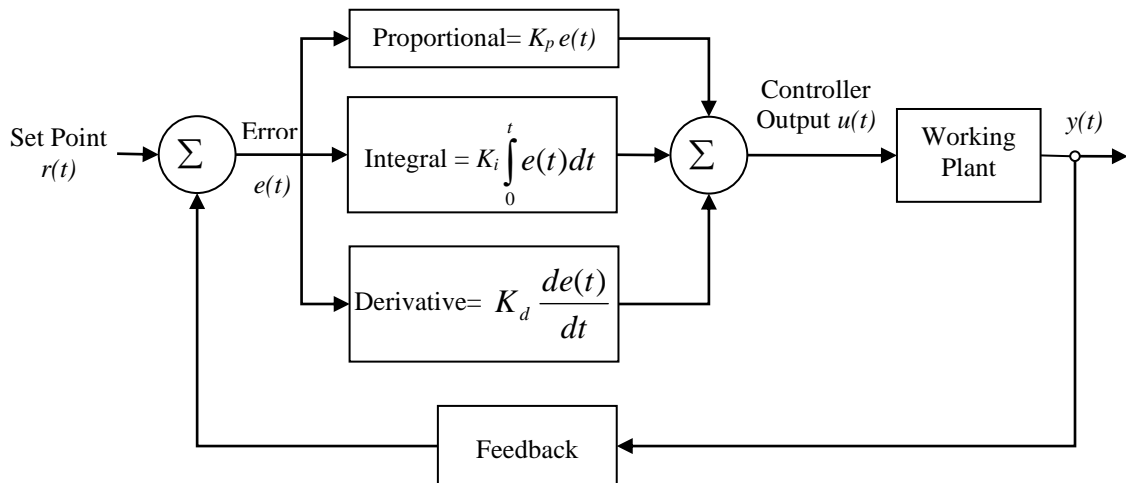

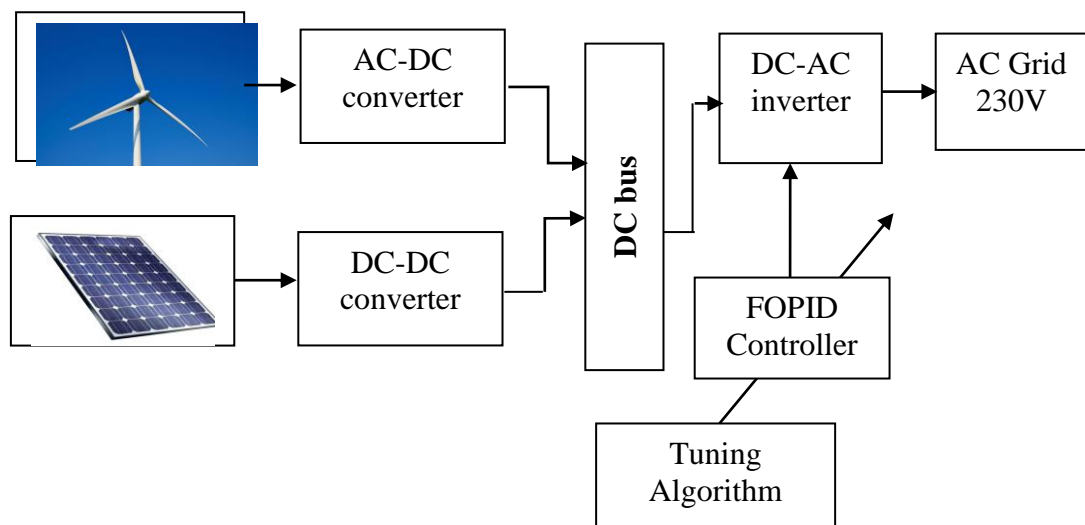**Figure 1:** Architecture of Conventional PID Controller

Figure 2: Architecture of FOPID Controller for Proposed System

III. Tuning Algorithm Used for PID and FOPID

There are three nature inspired algorithms used for the optimal tuning of proposed work. The details of all algorithms used are given below:

A. Fire Fly (FF) Algorithm

It is a nature-inspired optimization algorithm developed by Xin-She Yang in 2008. It works on flashing behavior of fireflies and their ability to attract each other through bioluminescent communication [24]. The main inspiration for the FF algorithm comes from the natural phenomenon where fireflies use their light to communicate and attract mates or prey [25]. The basic principle of working includes the following:

Attraction: The brightness is the feature behind the attractiveness of a firefly, which is directly associated with the objective function to be optimized and the brighter of the fireflies attracts others.

Light Intensity: The light intensity i.e. brightness of firefly diminishes with distance due to absorption in the medium. Therefore, fireflies are attracted to each other on the basis of their relative brightness, and the attraction decreases with increase in distance.

Movement: A firefly moves towards another brighter firefly on the basis of their brightness and their movement is highly influenced by the attractiveness, which decreases with distance which is subject to a randomization factor to provide exploration and avoid local optima [26].

The technique of this algorithm is described with the following steps:

Step 1: Initialization: Fist of all, define a objective function $f(x)$ to be minimized or maximized as per requirement, then initialize a population of fireflies with random positions in the search space. Set algorithm parameters by selecting number of fireflies n, maximum generations T, absorption coefficient γ, attractiveness β_0 at zero distance, and the randomization parameter is α.

Step 2: Light Intensity and Attractiveness: Calculate the light intensity I of each firefly based on their position x_i, where $I_i = f(x_i)$ for maximization problems or it can be $I_i = -f(x_i)$ for minimization problems. The attractiveness β of a firefly is $\beta(r) = \beta_0 e^{-\gamma r^2}$ where, r defines the distance between two fireflies.

Step 3: Calculate the Distance: The distance r_{ij} between two fireflies i and j is calculated using the Euclidean distance is given below:

$$r_{ij} = \left\| x_i - x_j \right\| = \sqrt{\sum_{k=1}^{d} (x_{i,k} - x_{j,k})^2} \tag{4}$$

In above, x is the kth component of the position for i^{th} firefly, and d is the dimensionality of the problem.

Step 4: Movement of Fireflies: The firefly i is attracted by another brighter firefly j and moves towards it. The movement is

$$x_i = x_i + \beta_0 e^{-\gamma r_{ij}^2} (x_j - x_i) + \alpha(rand - 0.5) \tag{5}$$

In above equation (5), α represents randomization parameter, and $rand$ is a random number which is uniformly distributed between [0,1].

Step 5: Update and Iteration: Now, update the positions of all the fireflies and evaluate the new positions and update the light intensities. Further, repeat this movement process for a set number of generations or until a convergence criterion is met [27] [28].

B. Path Finder (PF) Algorithm

It is a nature-inspired optimization algorithm modeled on the cooperative behavior of social animals which may be ants or bees. They navigate and work under a complex environment to find the shortest paths between their nests and food sources [29]. The PF algorithm works on the principles of swarm intelligence, including communication, cooperation, and the use of pheromone-like markers to guide the search process [30]. The basic steps for working principles of this algorithm are given below:

Step 1: Initialization: Firstly to define the optimization problem with an objective function $f(x)$, then initialize a population of agents (path finder) with random positions in the search space. Further, set the algorithm parameters like the number of agent's n, maximum iterations T, pheromone influence α, and heuristic information influence factor β.

Step 2: Update their Search Space: The agents or swarm deposit their virtual pheromones on their paths as they explore the search space with an intensity of the pheromone τ is updated based on the quality of the solution

found by the agents. They use heuristic information to guide agents towards promising areas of their search space. Then, each agent probabilistically chooses the next step on the basis of pheromone intensity and heuristic information. The probability function P_{ij} of their movement from position i to j is given by:

$$P_{ij} = \frac{(\tau_{ij})^\alpha (\eta_{ij})^\beta}{\sum_{k \in N_i} (\tau_{ik})^\alpha (\eta_{ij})^\beta} \qquad (6)$$

In above equation, where τ{ij} represents the pheromone intensity on path (i,j), η_i is the heuristic information, α and β are the parameters for controlling influence of pheromone and heuristic information, Ni represents the set of possible next steps from position i.

Step 3: Path Selection and Update: When each agent completes its path, then it updates the pheromone trails:

$$\tau_{ij} = (1-\rho)_j + \Delta\tau_{ij} \qquad (7)$$

In above equation (7), ρ is the pheromone evaporation rate and $\Delta\tau_{ij}$ is the amount of pheromone deposited by the agents which is often related to the quality of the solution obtained.

Step 4: Iteration and Convergence: Now, repeat the movement, path selection, and pheromone update processes for a set of iterations or until a convergence criterion is met, like a quality threshold solution or stagnation in improvements [31] [32].

C. Whale Optimization Algorithm (WOA)

It is also a nature-inspired optimization algorithm developed by Mirjalili and Lewis in 2016 which depends on social behavior of whales [33], particularly their hunting strategy called as bubble-net feeding. The algorithm is designed in order to solve optimization problems by modeling the bubble-net hunting mechanism mathematically [34]. The steps involved in this algorithm are given below:

Step 1: Initialization: There is initializing of population of whales with random positions in the search space. Then, set the algorithm parameters on the basis of number of whales' n, maximum number of iterations T, and constants A, C, and b.

Step 2: Update Position: In this for each whale, update the position using either the shrinking encircling mechanism or the spiral updating position on the basis of probability p.

If $p<0.5p<0.5$ then

$$\vec{X}(t+1) = \vec{X}*(t) - A \cdot DX$$

If $p \geq 0.5p \geq 0.5$ then

$$\vec{X}(t+1) = D' \cdot e^{bl} \cdot \cos(2\pi l) + \vec{X}*(t)$$

Step 3: Iteration and Convergence: Now, repeat the position updating process for each whale until a maximum number of iterations is reached or a convergence criterion is satisfied as per requirements [27] [35].

IV. RESULTS AND DISCUSSION

The proposed work has been performed in MATLAB in which there is an analysis for the performance comparison of traditional PID and FOPID controller. The proposed system consists of a grid specifically single phase which is integrated to solar PV and Wind Power enabled system. In this, there is performance comparison on DC link voltage and output voltage of proposed system. The FF, WOA and PF algorithm are used to optimally tune the PID and FOPID controller and their values are given in table 2. The overall analysis of voltage has been carried out corresponding to time. Moreover, the analysis has also been carried out on various parameters such as: "Rise time, Settling time, Settling Maximum, Settling Minimum, Overshoot, Undershoot, Peak and Peak time". The specifications of hybrid PV array along with wind energy are given below in table 1:

Table 1: Specifications of Proposed System

S. No.	Solar PV	Wind	AC/DC rectifier
1	Isc in Ampere: 2.02	Initial wind speed in m/s: 10	Snubber resistance: 105
2	Vsc in Volts: 86.8	Stator resistance in pu: 0.06	Diode resistance in Ω: 0.001
3	Im in Ampere: 1.93		Diode inductance in H: 0
4	Vm in Volts: 70.4		

A. Analysis of DC Link Voltage

In this, there is analysis of DC link voltage of grid connected solar wind system and output has been analysed using three different cases of solar irradiance and wind speed. In Case I, the value of Solar Irradiance is 850

W/m^2 & Wind Speed is 15 ms, in Case II, output is analysed at Solar Irradiance of 900 W/m^2 & Wind Speed is 10 ms and in Case III, output is analysed at Solar Irradiance of 1000 W/m^2 and Wind Speed is 15 ms. For the comparison point of view, both PID and FOPID DC link output has been taken into consideration.

Case 1: The figure 3 and figure 4 indicates the DC link voltage waveform at time of 0-1 second for the proposed solar wind based grid integrated system using PID and FOPID controller respectively. The DC link voltage responses in terms of "rise time, settling time, settling minimum, settling maximum, overshoot undershoot, peak and peak time" are given in table 3. The FF algorithm based controller has a moderately fast response of 0.295 Seconds which stabilizes quickly at 0.35 seconds. The WOA based PID controller yields a slightly faster rise time 0.282 seconds but have a significantly longer settling time 0.54 seconds. PF algorithm base controller has having fastest rise time (0.243 seconds) and the shortest settling time (0.335 seconds) amongst all PID controllers. The fast response means the system is very responsive with quick stabilization; as a result there is good balance between speed and stability. The FF controller with FOPID shows improved performance over the traditional PID controller, with both a quicker rise time 0.245 seconds and shorter settling time 0.32 seconds. This indicates enhanced system stability and faster response to changes. WOA optimized FOPID controller provides the fastest rise time 0.22 seconds amongst all the listed methods, but with a longer settling time as compared to PF-FOPID. PF-FOPID controller shows a slightly slower rise time 0.235 seconds than WOA-FOPID but a comparable settling time of 0.37 seconds.

Overshoot means the extent to which the system exceeds the desired value at its transient response. FF based PID has an overshoot of 0.058 which indicates that the system exceeds the desired set point by 5.8%. WOA optimized PID controller has a slightly lower overshoot of 0.056 (5.6%). This indicates a slight improvement in terms of reducing overshoot as compared to FF-PID, suggesting better stability and control performance. PF tuned PID controller has an overshoot of 0.0586 (5.86%). This is slightly higher than both FF-PID and WOA-PID. The FF algorithm tuned FOPID has an overshoot of 0.0572 (5.72%) which is slightly lower than the FF-PID controller, suggesting that the fractional order control improves system stability and reduces overshoot. The WOA optimized FOPID controller has an overshoot of 0.0567 (5.67%). The PF tuned FOPID controller has the lowest overshoot of 0.0563 (5.63%) amongst all methods used.

Case II: The figure 5 and the figure 6 indicate the DC link voltage waveform at time of 0-1 second using PID and FOPID controller. The DC link voltage responses are given in table 4. The FF-PID configuration shows a moderate rise time of 0.22 seconds but has the longest settling time (0.388 seconds) and the highest overshoot (0.0593). The WOA-PID configuration has the fastest rise time (0.197 seconds) and the lowest overshoot (0.055) but the longest settling time (0.538 seconds) which implies that it responds quickly but takes a while to stabilize fully due to oscillations. The PF-PID provides a fast rise time (0.198 seconds) and the shortest settling time (0.32 seconds) with a moderate overshoot (0.06) which means it is a well-balanced controller with quick response and stabilization.

The FF based FOPID has a fast rise time (0.21 seconds), moderate settling time (0.29 seconds) and moderate overshoot (0.0537) which reflects that there is improved stability and responsiveness as compared to PID. The WOA based FOPID offers a moderate rise time (0.215 seconds), the shortest settling time (0.28 seconds), and low overshoot (0.0536) which is a clear indication of good balanced system with quick response and stability with minimal oscillations. PF-FOPID has the slowest rise time (0.218 seconds) among FOPID controllers but the lowest overshoot (0.0529), indicating it is the most stable with minimal overshoot but takes slightly longer (0.31 seconds) to respond initially and stabilize. Thus, all the controllers which used WOA based FOPID provides best overall performance with a good balance of fast response and stability.

Case III: The figure 7 and figure 8 indicates the DC link voltage waveform at time of 0-1 second using PID and FOPID controller respectively. The DC link voltage responses are given in table 5. The FF-PID has the fastest rise time (0.207 seconds) and shortest settling time (0.3 seconds) among PID controllers, but it comes at the cost of the highest overshoot (0.068), indicating potential instability and higher oscillations. WOA-PID has the slowest rise time (0.24 seconds and longest settling time (0.52 seconds) but the lowest overshoot (0.0527), indicating a stable but slower response with minimal oscillations. PF-PID provides a balance between rise time (0.215 seconds) and settling time (0.35 seconds) but has the highest overshoot (0.068).

The achieved value of rise time (0.227 seconds) and the shortest settling time (0.28 seconds) among FOPID controllers by FF-PID, with moderate overshoot (0.0559). WOA-FOPID offers the fastest rise time (0.21 seconds) among FOPID controllers, but with the longest settling time (0.35 seconds) and moderate overshoot (0.0556). PF-FOPID has the slowest rise time (0.23 seconds) among FOPID controllers but with moderate settling time (0.32 seconds) and the lowest overshoot (0.0551), indicating the best stability and minimal

oscillations. Hence, from the above analysis, it has been observed that the FOPID controllers demonstrate better performance in terms of stability (lower overshoot) as compared to PID controllers.
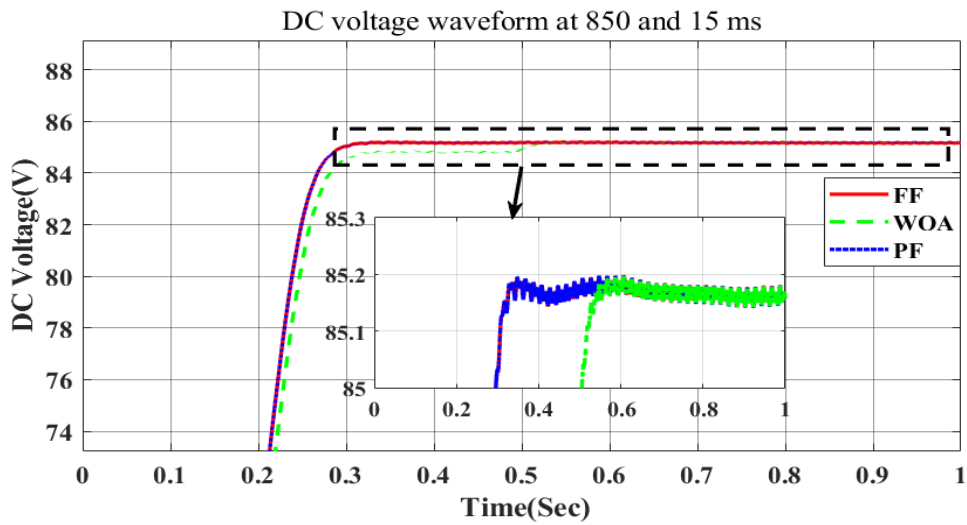

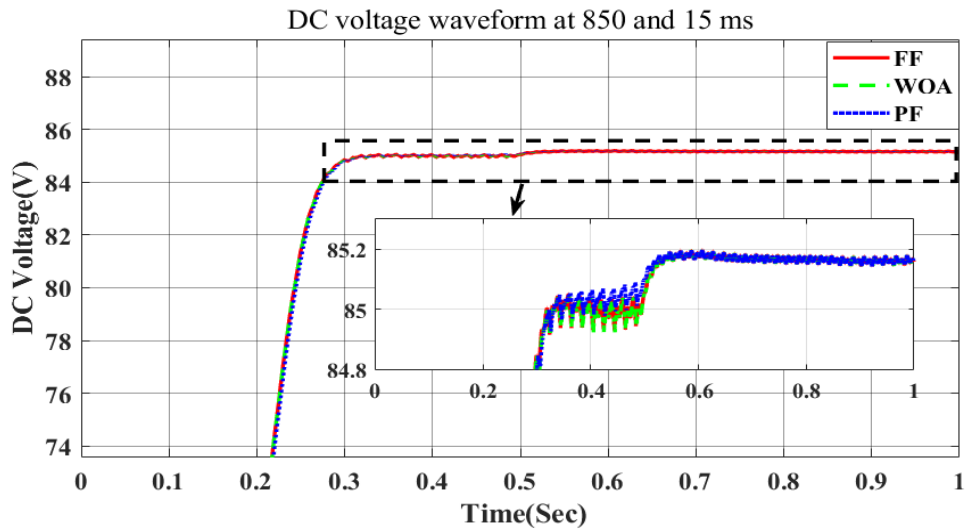**Figure 3:** DC link voltage for PID at Solar Irradiance (850 W/m^2) and Wind Speed (15 ms)

Figure 4: DC link voltage for FOPID at Solar Irradiance (850 W/m^2) and Wind Speed (10ms)
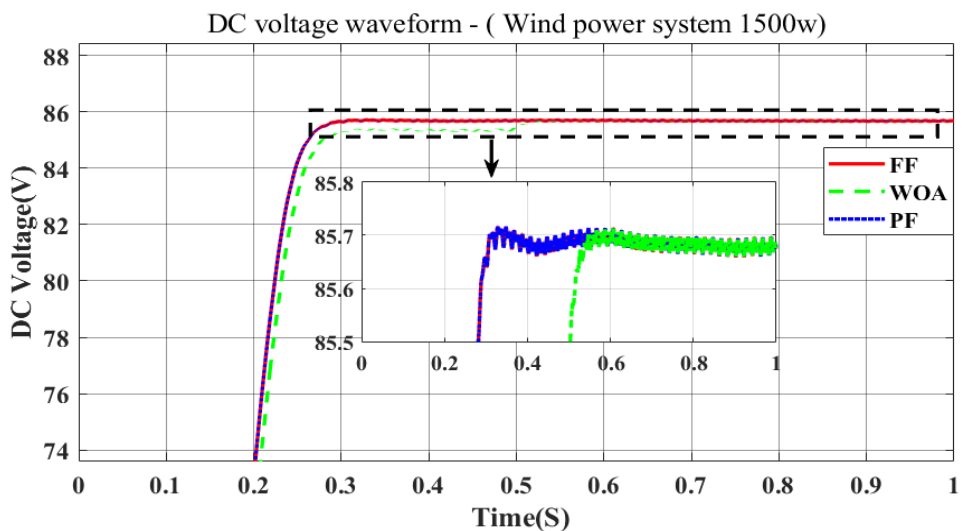

Figure 5: DC link voltage for PID at Solar Irradiance (900 W/m^2) and Wind Speed (10ms)
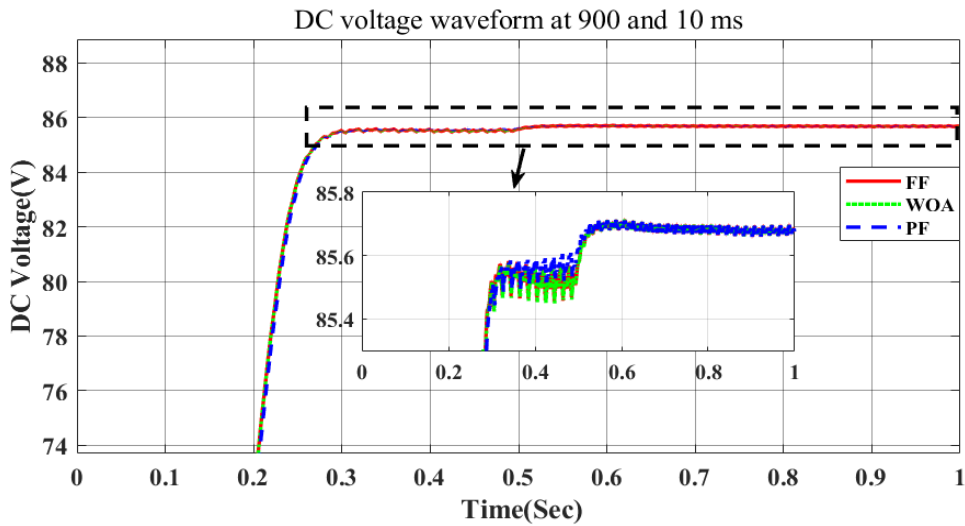
Figure 6: DC link voltage for FOPID at Solar Irradiance (900 W/m^2) and Wind Speed (10 ms)
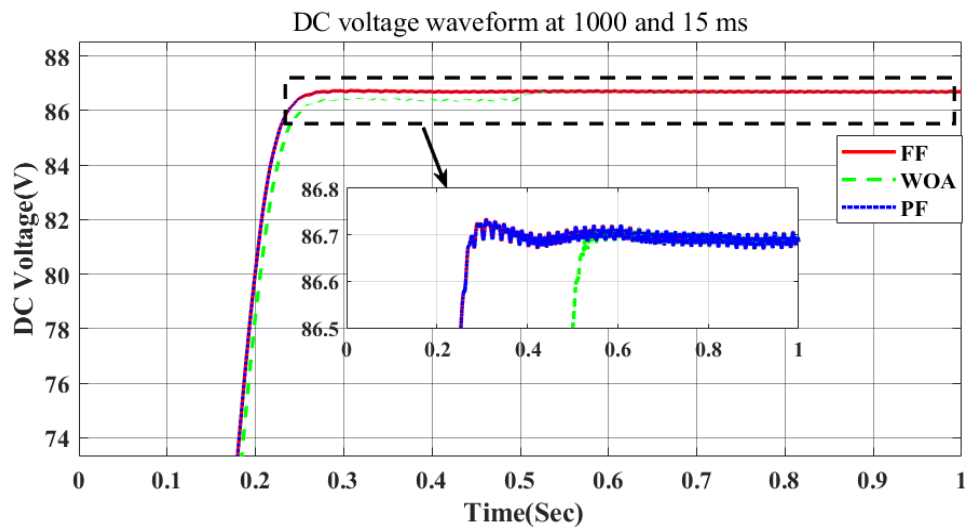

Figure 7: DC link voltage for PID at Solar Irradiance (1000 W/m^2) and Wind Speed (15 ms)
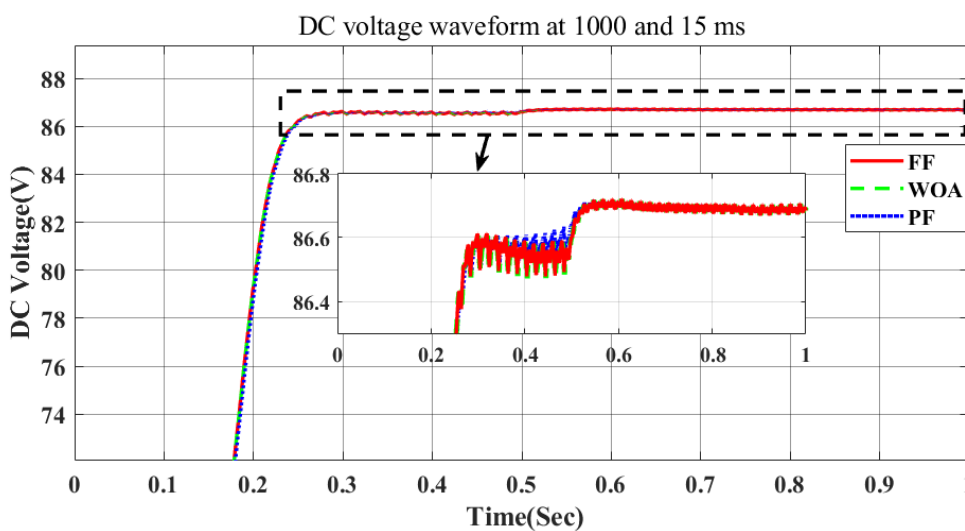

Figure 8: DC link voltage for FOPID at Solar Irradiance (1000 W/m^2) and Wind Speed (15 ms)

B. Analysis of Output Voltage

The figures from figure 9 to figure 14 shows the grid connected inverter's output under Case III at Solar Irradiance of 1000 W/m^2 and Wind Speed of 15 ms. The waveform represents the output voltage of PID and

FOPID controller with FF, WOA & PF algorithm. In each case, the considered peak to peak value of voltage is 230 V.
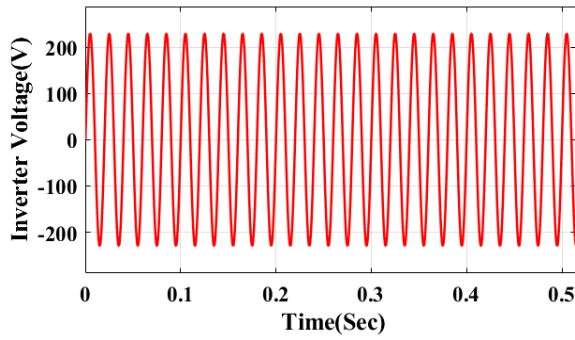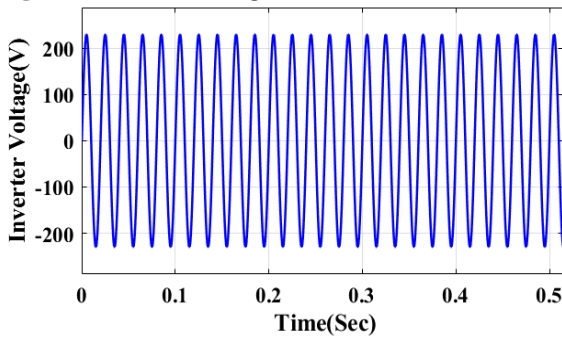

Figure 9: Inverter voltage for FF based PID

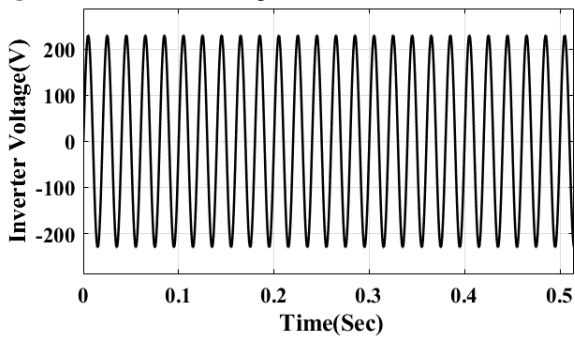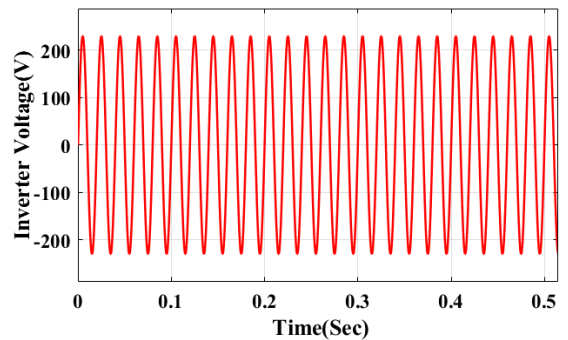**Figure 12:** Inverter voltage for FF based FOPID

Figure 10: Inverter voltage for PF based PID

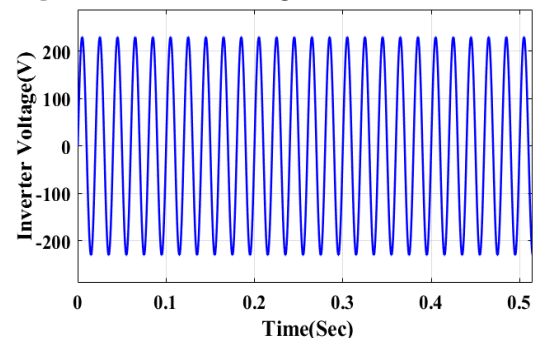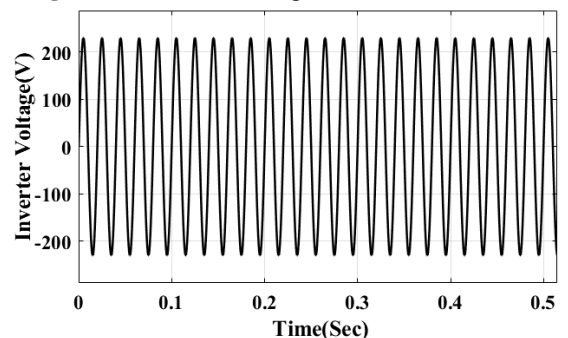**Figure 13:** Inverter voltage for PF based FOPID

Figure 11: Inverter voltage for WOA based PID

Figure 14: Inverter voltage for WOA based FOPID

Table 2: Values of PID and FOPID Parameters for Tuning

Parameters	PID Firefly (FF)	PID Path Finder (PF)	PID Whale Optimization Algorithm (WOA)	FOPID Firefly (FF)	FOPID Path Finder (PF)	FOPID Whale Optimization Algorithm (WOA)
Kp	1.627	-2.1984	3.0721	-10	2.045	-3.027
Ki	42.3862	4.978	4.5175	-0.66015	4.5458	-6.8886
Kd	0	0.45308	9.7224	-8.5442	-4.225	-3.935
Lamda (λ)				1.2483	0.4587	1.6972
Mu (μ)				2	0.2556	1.4891

Table 3: DC Link voltage response of system at Solar Radiation 850 W/m² and Wind Speed 15 ms

	FF-PID	WOA-PID	PF-PID	FF-FOPID	WOA-FOPID	PF-FOPID
Rise Time	0.295	0.282	0.243	0.245	0.22	0.235
Settling time	0.35	0.54	0.335	0.32	0.38	0.37
Overshoot	0.058	0.056	0.0586	0.0572	0.0567	0.0563
Settling Min	85.140	85.141	85.140	85.141	85.1414	85.1416
Settling Max	85.198	85.197	85.1986	85.1982	85.1981	85.1979
Overshoot	0.058	0.056	0.0586	0.0572	0.0567	0.0563
Undershoot	0	0	0	0	0	0
Peak	85.1986	85.197	85.1986	85.1982	85.1981	85.1979
Peak time	0.605	0.53	0.60	0.359	0.3602	0.483

Table 4: DC Link voltage response of system at Solar Radiation 900 W/m^2 and Wind Speed 10 ms

	FF-PID	WOA-PID	PF-PID	FF-FOPID	WOA-FOPID	PF-FOPID
Rise Time	0.22	0.197	0.198	0.21	0.215	0.218
Settling time	0.388	0.538	0.32	0.29	0.28	0.31
Settling Min	85.6576	85.658	85.657	86.6677	86.6679	86.6681
Settling Max	85.7169	85.713	85.717	86.7214	86.7213	86.7210
Overshoot	0.0593	0.055	0.06	0.0537	0.0536	0.0529
Undershoot	0	0	0	0	0	0
Peak	85.7169	85.713	85.717	86.7214	86.7213	86.7210
Peak time	0.342	0.621	0.329	0.318	0.319	0.48

Table 5: DC Link voltage response of system at Solar Radiation 1000 W/m^2 and Wind Speed 15 ms

	FF-PID	WOA-PID	PF-PID	FF-FOPID	WOA-FOPID	PF-FOPID
Rise Time	0.207	0.24	0.215	0.227	0.21	0.23
Settling time	0.3	0.52	0.35	0.28	0.35	0.32
Settling Min	86.6676	86.6682	86.6676	85.658	85.6581	85.6584
Settling Max	86.7356	86.7209	86.7356	85.7139	85.7137	85.7135
Overshoot	0.068	0.0527	0.068	0.0559	0.0556	0.0551
Undershoot	0	0	0	0	0	0
Peak	86.7356	86.7209	86.7356	85.7139	85.7137	85.7135
Peak time	0.308	0.606	0.3085	0.339	0.34	0.483

V. CONCLUSION

This paper proposed a comparative analysis of PID and FOPID controller configurations using different tuning algorithm for single phase grid connected solar PV and wind power plant. The performance of all in terms of DC link voltage with their responses is highlighted significantly. The differences in their performance metrics are very crucial in determining the best controller for specific application needs. There are three proposed cases depending on solar irradiance and wind speed on which the system is tested. Under case I, PF-FOPID stands out for its superior stability with the lowest overshoot 0.0563 while WOA-FOPID offers the fastest rise time 0.22 seconds. FF-FOPID achieves the quickest stabilization in 0.32 seconds. In case II, WOA based FOPID provides the best overall performance with a good balance of fast response and stability. In case III, PF-FOPID provides the best overall performance with minimal overshoot which is the clear indication of its superiority in terms of stability; whereas, FF-FOPID achieved stability in smallest time period. From the obtained experimental results, it has been observed that the FOPID controllers generally provide better overall performance in terms of stability and settling time as compared to PID controllers. Hence, it has been concluded that the selection of a controller should be selected on the basis of specific requirements or application.

REFERENCES

[1] I. Pan and S. Das, "Fractional-order AGC for distributed energy resources using robust optimization," IEEE Transactions on Smart Grid, vol. 7, no. 5, pp. 2175-2186, Sep. 2016.

[2] S. Li, D. Xu, and L. He, "Performance evaluation of classical and fractional-order PI controllers for a speed control system," IEEE Transactions on Control Systems Technology, vol. 25, no. 4, pp. 1399-1410, July 2017.

[3] M. Rahman, et al., "Design of PID Controller with Grid Connected Hybrid System," Springer, 2023.

[4] N. Pham, et al., "Adaptive Fractional Order PID Controller Based MPPT for PV Connected Grid System," Springer, 2023.

[5] H. K. Liu, et al., "Design of Cascaded PI-Fractional Order PID Controller for Improving the Frequency Response of a Hybrid Microgrid System," IEEE Transactions on Power Systems, vol. 38, no. 1, pp. 84-94, Jan. 2023.

[6] J. Lee, et al., "Grid Integration Challenges and Solution Strategies for Solar PV and Wind Power Systems," IEEE Transactions on Sustainable Energy, vol. 14, no. 2, pp. 593-603, April 2023.

[7] Deekshitha S. Nayak, R. Shivarudraswamy, and Florent Drossard, "The New Control Scheme for the PV and Wind Hybrid System Connected to the Single Phase Grid," Journal of Electrical Engineering & Technology, vol. no. 15, pp.1929-1936, 2020.

[8] A. Ahmad, L. Rajaji, and A. Iqbal, "A novel current controller design for grid-integrated PV inverter system," SN Applied Sciences, vol. no. 3, 323, 2021.

[9] Gaddala Jayaraju and Gudapati Sambasiva Rao, "A New Optimized ANN Algorithm Based Single Phase Grid Connected PV-Wind System Using Single Switch High Gain DC-DC Converter," European Journal of Electrical Engineering, Vol. 21, No. 4, pp. 373-381, 2019.

[10] Aurobinda Panda, M K Pathak, and S P Srivastava, "A single phase photovoltaic inverter control for grid connected system," Indian Academy of Sciences, vol. 41, no. 1, pp. 15-30, January 2016.

[11] M. A. George, D. V. Kamat, and C. P. Kurian, "Electric vehicle speed tracking control using an ANFIS-based fractional order PID controller," Journal of King Saud University – Engineering Sciences, 2022.

[12] S. M. A. Altbawi, A. S. B. Mokhtar, T. A. Jumani, I. Khan, N. N. Hamadneh, and A. Khan, "Optimal design of Fractional order PID controller based Automatic voltage regulator system using gradient-based optimization algorithm," *Journal of King Saud University – Engineering Sciences*, vol. 36, no. 1, pp. 32-44, Jan. 2024.

[13] Rosy Pradhan, Santosh Kumar Majhi, Jatin Kumar Pradhan, Bibhuti Bhusan Pati, "Optimal Fractional Order PID Controller Design Using Ant Lion Optimizer," Ain Shams Engineering Journal, vol. 11, pp. 281-291, 2020.

[14] Hossam Kotb, Ahmed H. Yakout, Mahmoud A. Attia, Rania A. Turky, Kareem M. Aboras, "Speed Control and Torque Ripple Minimization of SRM Using Local Unimodal Sampling and Spotted Hyena Algorithms-Based Cascade PID Controller,Ain Shams Engineering Journal," Ain Shams Engineering Journal, vol. 13, p. 101719, 2022.

[15] Rui Yang, Yongbao Liu, Youhong Yu, Xing He, Hongsong Li, "Hybrid Improved Particle Swarm Optimization Cuckoo Search Optimized Fuzzy PID Controller for Micro Gas Turbine," Energy Reports, vol. 7, pp. 5446-5454, 2021.

[16] K. J. Åström and T. Hägglund, "PID Controllers: Theory, Design, and Tuning," 2nd ed., Instrument Society of America, 1995.

[17] J. G. Ziegler and N. B. Nichols, "Optimum Settings for Automatic Controllers," Transactions of the ASME, vol. 64, no. 11, pp. 759-768, Nov. 1942.

[18] K. Ogata, "Modern Control Engineering," 5th ed., Prentice Hall, 2010.

[19] C. A. Smith and A. B. Corripio, "Principles and Practice of Automatic Process Control," 3rd ed., Wiley, 2005.

[20] I. Podlubny, "Fractional-Order Systems and Fractional-Order Controllers," Institute of Experimental Physics, Slovak Academy of Sciences, Kosice, Slovak Republic, 1994.

[21] I. Podlubny, "Fractional-Order Systems and $PI\lambda D\mu$-Controllers," IEEE Transactions on Automatic Control, vol. 44, no. 1, pp. 208-214, Jan. 1999.

[22] K. Singh, S. Saroha, and A. Verma, "An Analysis on Integration of Solar and Wind Power into A Single-Phase Grid with an Optimal Parameterized Fractional-Order PID Controller," *Journal of Electrical Systems*, vol. 20, no. 1s, Mar. 2024.

[23] K. Singh, S. Saroha, A. Verma, P. Prabhakar, K. Kumar, and C. Madan, "An Optimal Parameterized Fractional-Order PID Controller for the Single Phase Grid Integrated with Solar and Wind System," *Cybernetics and Systems*, vol. 54, no. 7, pp. 1086-1110, 2023.

[24] X.-S. Yang, "Firefly Algorithm, Stochastic Test Functions and Design Optimization," International Journal of Bio-Inspired Computation, vol. 2, no. 2, pp. 78-84, 2010.

[25] X.-S. Yang, "Firefly Algorithm for Multimodal Optimization," in "Stochastic Algorithms: Foundations and Applications," SAGA 2009, Lecture Notes in Computer Science, vol. 5792, O. Watanabe and T. Zeugmann, Eds. Springer, Berlin, Heidelberg, pp. 169-178, 2009.

[26] X.-S. Yang, "Firefly Algorithm, Levy Flights and Global Optimization," in "Research and Development in Intelligent Systems XXVI," M. Bramer, R. Ellis, and M. Petridis, Eds. Springer, London, pp. 209-218, 2010,.

[27] X.-S. Yang, "Nature-Inspired Metaheuristic Algorithms," 2nd ed., Luniver Press, 2010.

[28] M. S. Gandomi, X.-S. Yang, A. H. Alavi, and S. Talatahari, "Firefly Algorithm with Chaos," Communications in Nonlinear Science and Numerical Simulation, vol. 18, no. 1, pp. 89-98, Jan. 2013.

[29] M. Dorigo and T. Stützle, "Ant Colony Optimization," MIT Press, 2004.

[30] C. Blum and X. Li, "Swarm Intelligence in Optimization," in "Handbook of Swarm Intelligence," Springer, Berlin, Heidelberg, 2011, pp. 43-85.

[31] M. G. H. Omran, A. P. Engelbrecht, and A. Salman, "Particle Swarm Optimization Method for Image Clustering," International Journal of Pattern Recognition and Artificial Intelligence, vol. 19, no. 3, pp. 297-321, 2005.

[32] E. Bonabeau, M. Dorigo, and G. Theraulaz, "Swarm Intelligence: From Natural to Artificial Systems," Oxford University Press, 1999.

[33] S. Mirjalili and A. Lewis, "The Whale Optimization Algorithm," Advances in Engineering Software, vol. 95, pp. 51-67, May 2016.

[34] S. Mirjalili, S. M. Mirjalili, and A. Lewis, "Grey Wolf Optimizer," Advances in Engineering Software, vol. 69, pp. 46-61, Mar. 2014.

[35] X. Cai, Z. Cui, J. Zeng, and A. G. Luo, "Nature-Inspired Computation and Swarm Intelligence: Algorithms, Theory, and Applications," Elsevier, 2020.